Marie Skłodowska-Curie (MSCA) – Innovative Training Networks (ITN)
H2020-MSCA-ITN European Training Networks

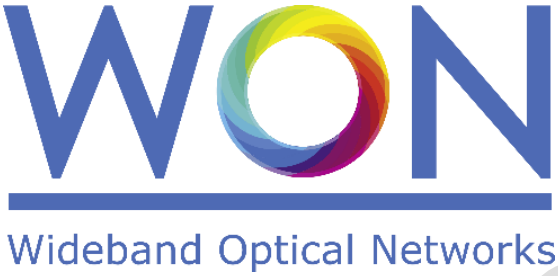

Wideband Optical Networks [WON]

Grant agreement ID: 814276

WP2 – Digital signal processing and system modelling

Deliverable D2.5 Experimental validation DSP techniques for wideband optical systems

This project has received funding from the European Union's Horizon 2020 research and innovation programme under the Marie Skłodowska-Curie grant agreement 814276.

Document Details

Work Package	WP2 – Digital signal processing and system modelling
Deliverable number	D2.5
Deliverable Title	Experimental validation DSP techniques for wideband optical systems
Lead Beneficiary:	Politecnico di Torino (PoliTo)
Deliverable due date:	30 June 2023
Actual delivery date:	26 June 2023
Dissemination level:	Public

Project Details

Project Acronym	WON
Project Title	Wideband Optical Networks
Call Identifier	H2020-MSCA-2018 Innovative Training Networks
Coordinated by	Aston University, UK
Start of the Project	1 January 2019
Project Duration	48 months
WON website:	https://won.astonphotonics.uk/
CORDIS Link	https://cordis.europa.eu/project/rcn/218205/en

WON Consortium and Acronyms

Consortium member	**Legal Entity Short Name**
Aston University	Aston
Danmarks Tekniske Universitet	DTU
VPIphotonics GmbH	VPI
Infinera Portugal	INF PT
Fraunhofer HHI	HHI
Politecnico di Torino	POLITO
Technische Universiteit Eidhoven	TUE
Universiteit Gent	UG
Keysight Technologies	Keysight
Finisar Germany GmnH	Finisar
Orange SA	Orange
Technische Universitaet Berlin	TUB
Instituto Superior Tecnico, University of Lisboa	IST

Abbreviations

CPR:	Carrier phase recovery
CRF:	Coherent receiver front-end
DA:	Driver amplifiers
DAC:	Digital to analog converter
DP:	Dual-polarization
DPD:	Digital pre-distortion
DSP:	Digital signal processing
ECL:	External cavity laser
EDFA:	Erbium-doped fiber amplifier
FF:	Frequency-flat
FO:	Frequency offset
FOC:	Frequency offset compensation
FS:	Frequency-selective
GSOP:	Gram-Schmidt orthonormalization procedure
LMS:	Least mean square
LO:	Local oscillator
MBT:	Multi-band transmission
OSNR:	Optical signal-to-noise ratio
QAM:	Quadrature amplitude modulation
RD:	Radius-directed
ROADM:	Reconfigurable Optical Add-drop Multiplexers
RTO:	Real-time oscilloscope
Rx:	Receiver
TDFA:	Thulium-doped fiber amplifier
Tx:	Transmitter
UWB:	Ultra-wide band

CONTENTS

LIST OF FIGURES

EXECUTIVE SUMMARY

The present scientific deliverable is part of Work Package 2 “Digital signal processing and system modelling”, in turn part of the ETN project WON “Wideband Optical Networks”, funded under the Horizon 2020 Marie Skłodowska-Curie scheme Grant Agreement 814276.

This document provides details on experimental validation of the usage of C-band transceivers applied to multi-band transmission (MBT) systems, ranging from the L- to S-band. The operational bandwidth of these devices can be relaxed by additional digital signal processing (DSP) techniques if the wavelength-dependency of these devices is properly characterized. For this scenario, the effectiveness of a cost-effective strategy for transceiver impairment mitigation and monitoring is shown and validated. This validation is achieved using a reduced-complexity DSP that makes use of standard wavelength-independent calibration. The work described in this document, including the results from experiments and offline DSP, have been generated in a collaboration between VPIphotonics and Fraunhofer HHI [1], [2].

1. Introduction

The continuous rise in traffic required by optical networks arises due to continually increasing IP traffic, along with the imminent deployment of 5G services, will require financially sustainable and cost-efficient capacity increases, preferably by maximizing usage of already-deployed infrastructure. One possible solution is multi-band transmission (MTB) [3], or ultra-wide band (UWB), systems, expanding the fiber spectral usage, which currently uses a 4.8 THz spectral window in the C-band. This solution has the advantage of not requiring deployment of new fiber spans and can be combined with higher-order modulation formats, to maximize data rate per wavelength. In any case, this solution requires new devices, such as amplifiers and Reconfigurable Optical Add-drop Multiplexers (ROADMs), which are being developed or are in the initial stages of deployment. Transceivers must also enable transmission within new wideband wavelengths; currently commercial solutions exist for C+L systems, but not for the S-band.

In this context, it is essential to understand the wavelength-dependency of the I/Q imbalance of C-band transceivers working outside of their manufacturing range [1] and, more importantly, to assess possible compensation schemes and resulting performance penalties. In [4] it is demonstrated that the C-L-band reception of 64 Gbaud, dual-polarization (DP) quadrature amplitude modulation (QAM)-32 and 64 signals is possible using off-the-shelf C-band components, performing only single-wavelength identification and predistortion. In this work, we summarize the results of [2], which identifies the variation of the frequency-resolved I/Q imbalance inside the signal electrical bandwidth versus wavelength for the C-band transceivers working in the L-C-S-bands, ranging from 1460 to 1608.8 nm. The monitoring is performed for transmitter (Tx) and receiver (Rx) I/Q for both amplitude and phase imbalance, together with I/Q skew up to half the Nyquist frequency. The observation shows the feasibility of cost-effective monitoring and compensation for the wavelength-dependency of the transceiver impairments in multi-band networks. Finally, we present the results of [1], presenting the impact of I/Q imbalances on maximum signal entropy, showing that practically penalty-free operation is preserved with a large margin in all the conditions considered.

2. Transceiver imbalance model and multi-band experimental setup

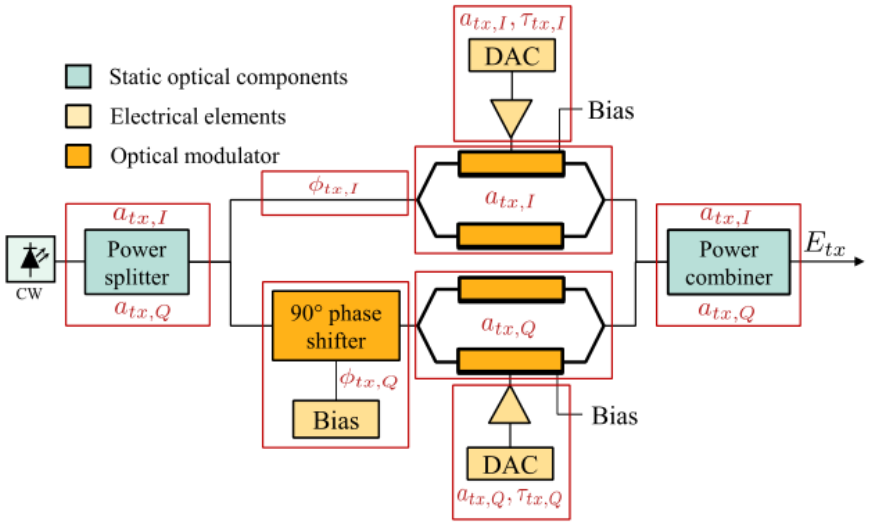

Figure 1: Single polarization transmitter model (Figure 1 of [2]).

Starting at the transmitter side, Figure 1 presents the general model of a single polarization optical transmitter, highlighting the sources of the different non-idealities. The baseband signal can be written as [5]:

$$u_{tx}(t) = a_{tx,I}\exp[j\phi_{tx,I}]\tilde{I}(t+\tau_{tx,I}) + ja_{tx,Q}\exp[j\phi_{tx,Q}]\tilde{Q}(t+\tau_{tx,Q})$$

Where $\tilde{I}$ and $\tilde{Q}$ are the ideal baseband in-phase and quadrature signals. Moreover, we can define the I/Q amplitude imbalance as $\gamma_{tx} = a_{tx,Q}/a_{tx,I}$, phase imbalance as $\Phi_{tx,I} = \phi_{tx,Q} - \phi_{tx,I}$ and I/Q skew as $\Delta\tau_{tx} = \tau_{tx,Q} - \tau_{tx,I}$. As the optical components operate in their designed wavelength range in the C-band, these elements are the main contributors for the I/Q imbalance, particularly the power splitter and combiner, which may present a wavelength-dependency, limiting system performance [6].

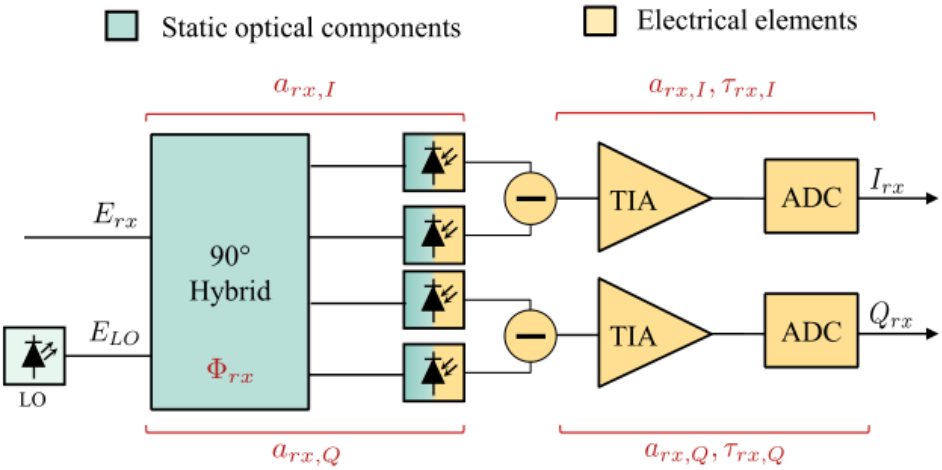

Figure 2: Single polarization receiver model (Figure 2 of [2]).

For the receiver side, shown in Figure 2, similarly to the transmitter, the I/Q amplitude imbalance is $\gamma_{rx} = a_{rx,Q}/a_{rx,I}$, the phase imbalance is $\Phi_{tx,I}$ and the I/Q skew is given by $\Delta\tau_{rx} = \tau_{rx,Q} - \tau_{rx,I}$. For this element, the electrical components introduce skew and contribute to the creation of an amplitude

imbalance. On the other hand, the optical components contribute to both phase and amplitude imbalances, mainly due to imperfections. Specially, the optical hybrids can present a large deviation from ideal performance when operating far from the design spectral region [1]. For simplicity, by assuming polarization alignment between the signal and the local oscillator (LO), the IQ signals can be written as [5]:

$$I_{rx}(t) \propto \mathrm{a}_{rx,I}[I(t)\cos(\Delta\omega t) - Q(t)\sin(\Delta\omega t)]$$
$$Q_{rx}(t) \propto \mathrm{a}_{rx,Q}[I(t)\sin(\Delta\omega t + \Phi_{rx}) + Q(t)\cos(\Delta\omega t + \Phi_{rx})] * \delta(t - \Delta\tau_{rx})$$

where $\Delta\omega$ is the frequency offset (FO) between the optical carrier and the LO, $\delta(\cdot)$ is the Dirac delta function, and $*$ is the convolution operator. It is visible from the above equation that the presence of a FO has the effect of rapidly mixing the I and Q signal components in time [5]. Furthermore, the FO separation results in a fundamental difference in the impact of Tx-side and Rx-side imbalance on system performance: while we can immediately compensate for Rx-side imbalance, Tx-side imbalance lies under the surface until carrier recovery is accomplished, affecting the performance of the whole DSP chain [2].

The experimental setup for the back-to-back characterization of the DP I/Q modulator and the coherent receiver is shown in
Figure 3. The 64 GBaud 32-QAM signals for the S-, C- and the L-band include Nyquist pulse shaping with a root-raised cosine at a roll-off of 0.1 [2]. The optical signals are generated by a commercially available C-band Lithium Niobate (LiNbO3) DP-I/Q modulator, together with an automatic bias control, to enable operation in an unstable wavelength range. An external cavity laser (ECL) is coupled with a thulium-doped fiber amplifier (for the S-band) or an erbium-doped fiber amplifier (EDFA) to provide the same power as a C-band laser, placed in front of the modulator. For the data source, a 120 GSa/s, 8-bit, 4 channel digital to analog converter (DAC) in combination with four linear driver amplifiers (DA) is used to create the electrical drive signal in front of the DP-I/Q modulator. For the LO used at the receiver, a LO-laser operating at 14 dBm is applied to the C- and L-bands, while for the S-band, a low-power laser amplified by a TDFA is used, operating at up to 16 dBm. The band amplification is performed only for C- and L-bands using two EDFAs (one for each band), due to the lack of a third TDFA [2]. In the absence of S-band amplification, this band presents a higher optical signal-to-noise ratio (OSNR) and an additional penalty. The OSNR, the effective SNR and signal power at the receiver are shown in Figure 4.

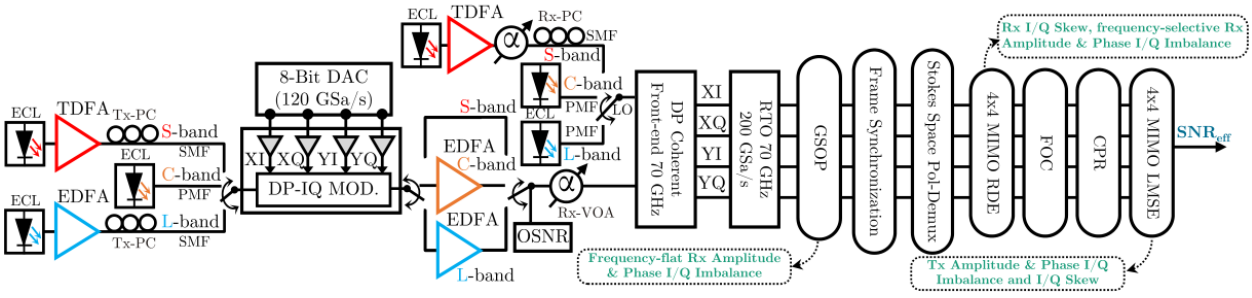

Figure 3: Experimental setup for back-to-back transmission for frequency-resolved I/Q imbalance characterization (Figure 3 of [2]).

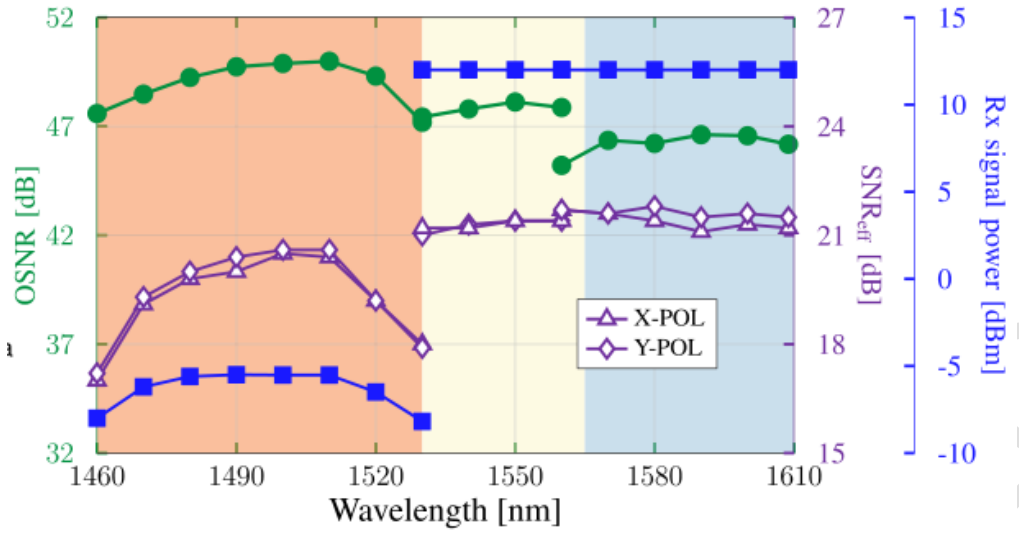

Figure 4: OSNR (green), effective SNR after DSP (purple), and received signal power (blue) versus wavelength (Figure 4 of [2]).

Before the coherent receiver front-end (CRF; from Fraunhofer HHI), a variable optical attenuator is applied to control the power. Moreover, four electrical analog outputs of the CRF are subsequently digitized at a sampling rate of 200 GSa/s using a 4-channel real-time oscilloscope (RTO) with 70 GHz analog electrical bandwidth and 8-bit resolution. The digitized signal is processed through data-aided DSP, designed to compensate the channel-induced impairments at an almost ideal level, and to provide a frequency-resolved characterization of the transceiver I/Q imbalance. After resampling, a Gram-Schmidt orthonormalization procedure (GSOP) is applied to compensate and monitor the frequency-flat amplitude and phase imbalance. The other stages consist of frame synchronization, a fully-data-aided equalizer with radius-directed (RD) adaptation to compensate and monitor Rx-side I/Q skew and frequency-selective amplitude and phase imbalance, frequency offset compensation (FOC), carrier phase recovery (CPR), and, finally, a post-equalizer based on fully-data-aided least mean square (LMS) adaptation is used to monitor the Tx-side I/Q imbalance. All additional details of the setup are presented in [2]. Finally, the received constellations at 1470, 1550 and 1600 nm are shown in
Figure 5, without and with GSOP compensation and equalization, showing the impact of the transceiver imperfections in different bands.

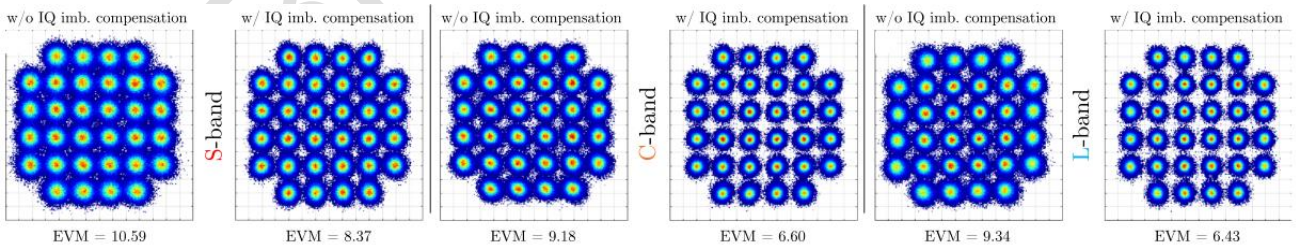

Figure 5: Received constellations after DSP at 1470 nm (S-band), 1550 nm (C-band), and 1600 nm (L-band) without and with GSOP compensationd and equalization (Figure 3 of [2]).

3. C-band receiver and transmitter characterizations for multi-band transmission

The I/Q imbalance can be described as the superposition of the frequency-flat (FF) and the frequency-selective (FS) components [7], in which are represented by $\bar{\gamma}$ (amplitude imbalance), $\overline{\Phi}$ (phase imbalance) and $\overline{\Delta\tau}$ (skew). The first characterization is performed for the receiver, which is done through the GSOP. The estimation was proven to be accurate in back-to-back as well as after transmission if $\Delta\omega\Delta\tau_{rx}$ is not large [1], [8]. In Figure 6 the FF I/Q amplitude and phase imbalance is presented. It is visible that, for both the amplitude and phase imbalance, the receiver presents a clear wavelength dependency. Regarding the amplitude imbalance, $\bar{\gamma}$ shows the highest value of ≈ 0.4 dB in the C-band (for X-polarization), while this value achieves ≈ 1.4 dB for the S-band (at 1460 nm), suggesting a higher dependency on the device fabrication imperfections outside the C-band. For the phase imbalance, is possible to see that, for the C-band window, the $\overline{\Phi}$ remains bellow $2°$ for both polarizations. Instead, this value increases up to $7°$ for the S-band. Moreover, the phase imbalance presents a linear trend for both polarizations with inverted slopes, which suggests a domination by a specific design of the optical dual-polarization $90°$-hybrid [2]. Even with this frequency-dependency, both amplitude and phase imbalance can be counteracted by the GSOP, resulting in a negligible system impact [1].

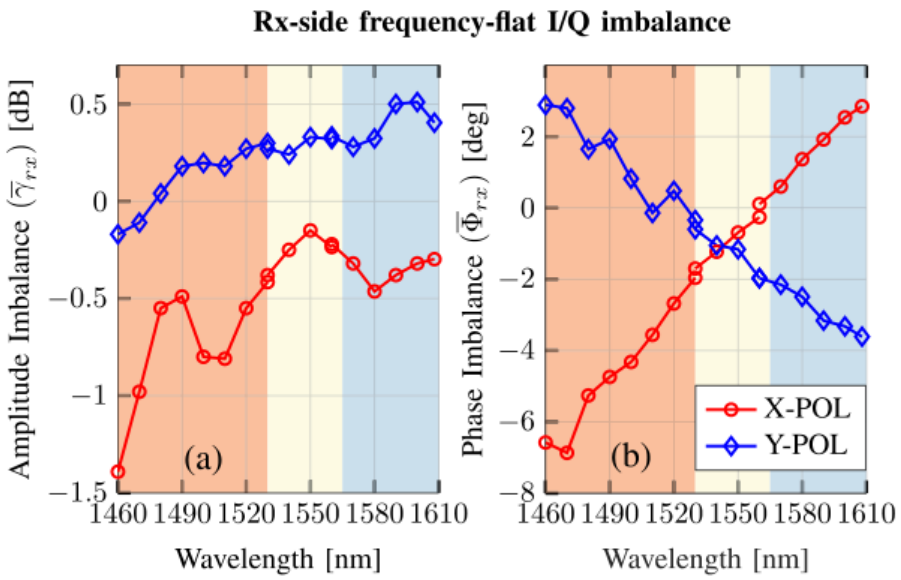

Figure 6: Receiver FF I/Q (a) amplitude, and (b) phase imbalance (Figure 5 of [2]).

Moving forward, in Figure 7 the FS imbalances and skew are presented for 5 wavelengths, 2 in the S-band (1470 and 1500 nm), 1 in the C-band (1550 nm), and 2 in the L-band (1570 and 1608.8 nm). For both amplitude and phase imbalance, it is possible to see that they do not have a significant difference between wavelengths, suggesting that the wavelength dependency impacts only the FF component [2]. This indicates that the GSOP was able to mitigate the FF imbalance, and the frequency-resolved calibration removed the FS imbalance. Moreover, the skew presented in Figure 7(e-f) is not wavelength-dependent, which is expected due to it being generated by electrical components.

The second characterization is performed for the transmitter, done after the carrier recovery from the post-equalizer. As in the receiver case, we present in Figure 8 the FF I/Q amplitude and phase

imbalance versus wavelength for the two polarizations. Regarding amplitude, the imbalance presents a flat behaviour with small values up to 0.35 dB. For phase imbalance, the plot also suggests no wavelength-dependency, with higher fluctuations if compared to the receiver amplitude imbalance. These results suggest the lack of degradation coming from power splitting and combining, and the effectiveness of the bias control applied for a MBT scenario [2].

Finally, in Figure 9 the FS amplitude and phase imbalance and skew are presented, again for five wavelengths. For all imperfections, a negligible wavelength variation is visible, suggesting that, due to the optical components operating in linearity, the wavelength-dependency is exclusive of the FF imbalance components. For the amplitude imbalance, the peak is around 18 GHz, with a slightly higher imbalance provided by Y-polarization. In any case, all values are within a ± 0.4 dB range, validating the effectiveness of the digital pre-distortion (DPD) that has been performed. Regarding the phase imbalance, its values remain up to $\approx 2°$, slightly higher than the values presented by the receiver. In any case, due to the wavelength-independence behaviour of the transmitter, a one-time additional calibration and compensation of extremely high-order modulation formats should be employed [9]. Lastly, even though the values where larger than the receiver, the skew shown does not present any critical behaviour.

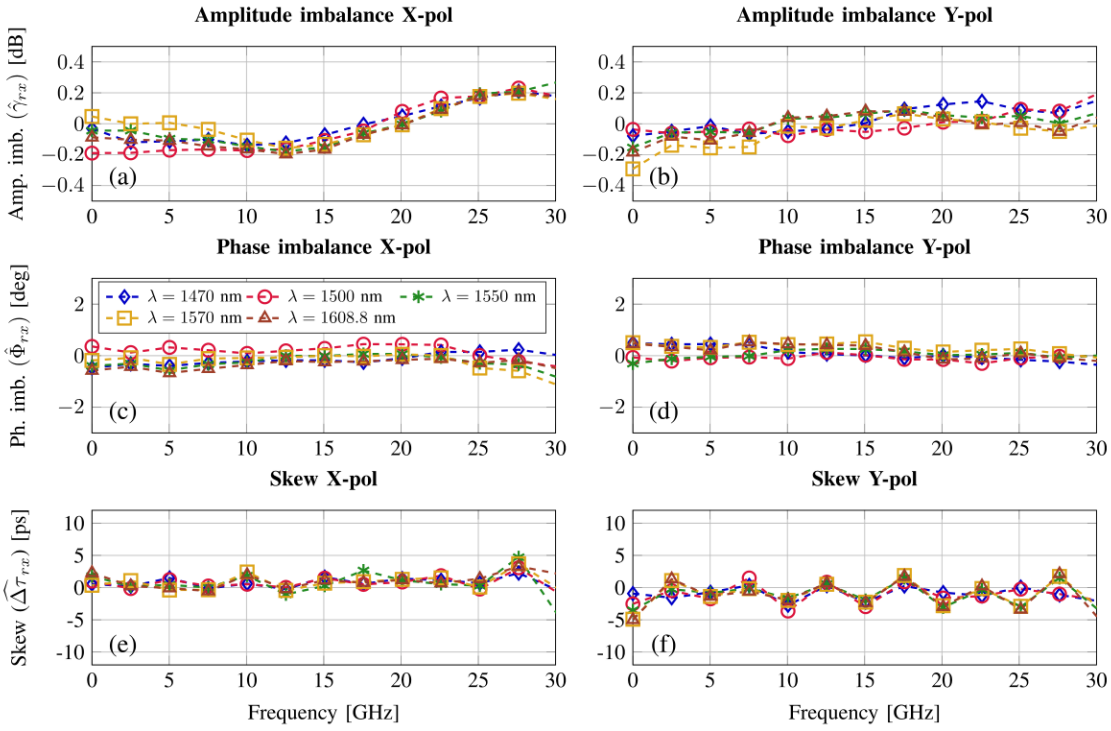

Figure 7: Receiver FS I/Q (a-b) amplitude, (c-d) phase imbalance, and (e-f) skew (Figure 6 in [2]).

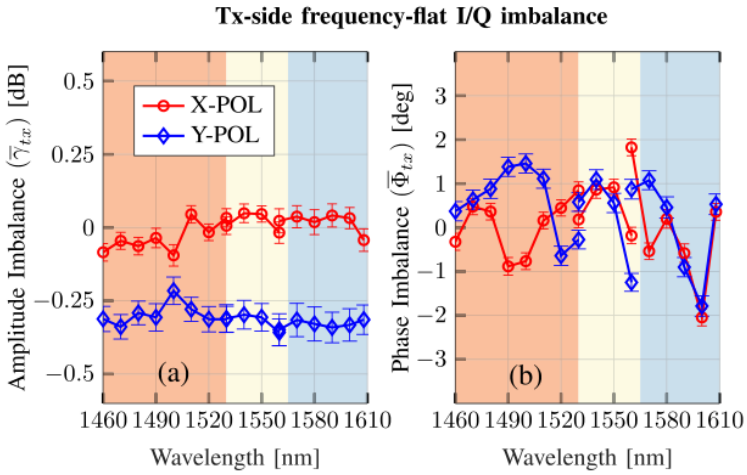

Figure 8: Transmitter FF I/Q (a) amplitude, and (b) phase imbalance (Figure 7 in [2]).

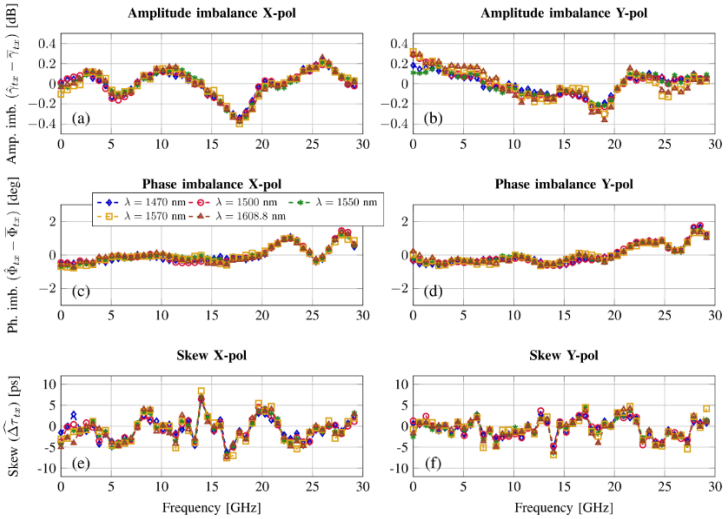

Figure 9: Transmitter FS I/Q (a-b) amplitude, (c-d) phase imbalance, and (e-f) skew (Figure 8 in [2]).

Finally, we show the simulation results presented in [1], which evaluate the impact of wavelength-dependency I/Q imbalance on signal entropy. The simulations are performed for 256/64 QAM-PS over an AWGN channel with received SNR of 20 and 15 dB, respectively. The results of Figure 10 show the sweep of Tx imbalances, from an ideal Rx to values much higher than the ones obtained by the previous characterization. By the results, even Tx-side imperfection presenting detrimental impact, is possible to see that almost penalty-free operation is preserved with a large margin in all considered conditions.

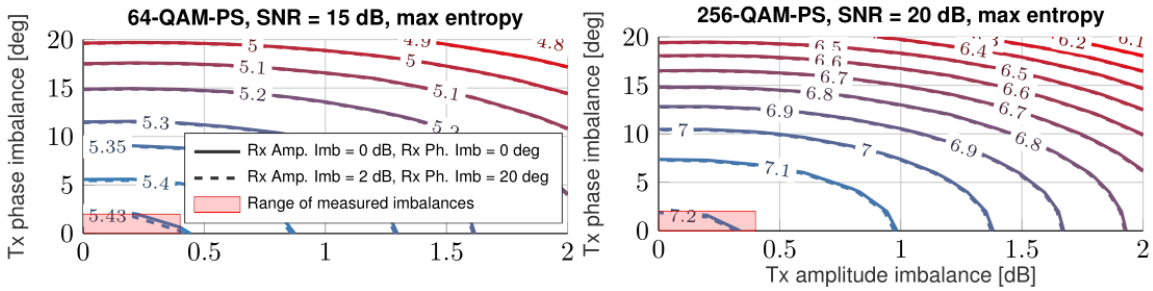

Figure 10: Achievable signal entropy versus transceiver I/Q imbalances (Figure 3 in [1]).

4. Conclusions

This work experimentally demonstrates the ability to make use of C-band commercial transceivers within a MBT scenario that ranges from the S- to L-bands. This demonstration is based on the characterization of the frequency-resolved I/Q imbalance versus the operating wavelength. This characterization has shown that, for the receiver, the wavelength variability is exclusively due to the FF component, which can be mitigated by standard digital compensations methods, for example, using a GSOP algorithm. For the transmitter, the characterization did not show any wavelength-dependency for the FF or FS imbalance, proving that these devices can be used for a wider range of wavelengths than the specified operating range. Moreover, the use of these devices for MBT scenarios should not require a costly wavelength-dependent calibration, DPD procedures or higher DSP complexity. These findings support the MBT as the most promising short-term solution to support the traffic increase required from optical networks.

5. REFERENCES

[1] G. D. Rosa, R. Emmerich, M. Sena, J. K. Fischer, C. Schubert und A. Richter, "Impact of Wavelength-Dependent I/Q Imbalances of Standard C-Band Transceivers in Rate-Adaptive Multiband Systems", in *2021 European Conference on Optical Communication (ECOC)*, 2021.

[2] G. Di Rosa, R. Emmerich, M. Sena, J. K. Fischer, C. Schubert, R. Freund und A. Richter, "Characterization, Monitoring, and Mitigation of the I/Q Imbalance in Standard C-Band Transceivers in Multi-Band Systems", *Journal of Lightwave Technology*, Bd. 40, Nr. 11, pp. 3470-3478, 2022.

[3] A. Napoli, N. Costa, J. K. Fischer, J. Pedro, S. Abrate, N. Calabretta, W. Forysiak, E. Pincemin, J. P.-P. Gimenez, C. Matrakidis, G. Roelkens und V. Curri, "Towards multiband optical systems" in *Advanced Photonics 2018 (BGPP, IPR, NP, NOMA, Sensors, Networks, SPPCom, SOF)*, 2018.

[4] R. Emmerich, M. Sena, R. Elschner, C. Schmidt-Langhorst, I. Sackey, C. Schubert und R. Freund, "Enabling S-C-L-Band Systems With Standard C-Band Modulator and Coherent Receiver Using Coherent System Identification and Nonlinear Predistortion", *Journal of Lightwave Technology*, Bd. 40, Nr. 5, pp. 1360-1368, 2022.

[5] J. Liang, Y. Fan, Z. Tao, X. Su und H. Nakashima,"Transceiver Imbalances Compensation and Monitoring by Receiver DSP", *Journal of Lightwave Technology*, Bd. 39, Nr. 17, pp. 5397-5404, 2021.

[6] M. Sena, Y. Cui, G. Fiol, B. Shariati, A. Napoli, J. K. Fischer, M. Schell und R. Freund, "Performance Evaluation of InP-Based DP-IQ Modulators for Multiband Transmission Systems", in *2020 22nd International Conference on Transparent Optical Networks (ICTON)*, 2020.

[7] A. Mohammadian und C. Tellambura, "RF Impairments in Wireless Transceivers: Phase Noise, CFO, and IQ Imbalance – A Survey", *IEEE Access*, Bd. 9, pp. 111718-111791, 2021.

[8] Y. Fan, Y. Jiang, J. Liang, Z. Tao, H. Nakashima und T. Hoshida, "Transceiver IQ imperfection Monitor by Digital Signal Processing in Coherent Receiver“, in *2019 24th OptoElectronics and Communications Conference (OECC) and 2019 International Conference on Photonics in Switching and Computing (PSC)*, 2019.

[9] D. Che und X. Chen, "Direct-Detection Based Frequency-Resolved I/Q Imbalance Calibration for Coherent Optical Transmitters“, in *Optical Fiber Communication Conference 2021*, 2021.